

MAGNETO-STATIC MODELLING OF THE MIXED PLASMA BETA SOLAR ATMOSPHERE BASED ON SUNRISE/IMAX DATA

T. WIEGELMANN¹, T. NEUKIRCH², D.H. NICKELER³, S.K. SOLANKI^{1,6}, V. MARTÍNEZ PILLET⁴, J.M. BORRERO⁵

¹Max-Planck-Institut für Sonnensystemforschung, Justus-von-Liebig-Weg 3, 37077 Göttingen, Germany, ²School of Mathematics and Statistics, University of St. Andrews, St. Andrews KY16 9SS, United Kingdom, ³Astronomical Institute, AV CR, Fricova 298, 25165 Ondrejov, Czech Republic, ⁴National Solar Observatory, Sunspot, NM 88349, USA, ⁵Kiepenheuer-Institut für Sonnenphysik, Schöneckstr. 6, 79104 Freiburg, Germany, ⁶School of Space Research, Kyung Hee University, Yongin, Gyeonggi, 446-701, Korea.

ApJ, accepted

ABSTRACT

Our aim is to model the 3D magnetic field structure of the upper solar atmosphere, including regions of non-negligible plasma beta. We use high-resolution photospheric magnetic field measurements from SUNRISE/IMaX as boundary condition for a magneto-static magnetic field model. The high resolution of IMaX allows us to resolve the interface region between photosphere and corona, but modelling this region is challenging for the following reasons. While the coronal magnetic field is thought to be force-free (the Lorentz-force vanishes), this is not the case in the mixed plasma β environment in the photosphere and lower chromosphere. In our model, pressure gradients and gravity forces are taken self-consistently into account and compensate the non-vanishing Lorentz-force. Above a certain height (about 2 Mm) the non-magnetic forces become very weak and consequently the magnetic field becomes almost force-free. Here we apply a linear approach, where the electric current density consists of a superposition of a field-line parallel current and a current perpendicular to the Sun's gravity field. We illustrate the prospects and limitations of this approach and give an outlook for an extension towards a non-linear model.

Subject headings: Sun: magnetic topology—Sun: chromosphere—Sun: corona—Sun: photosphere

1. INTRODUCTION

While the corona, at least above active regions, has a low plasma β and is usually modelled by the assumption of a vanishing Lorentz-force (see Wiegelmann & Sakurai 2012, for an overview of solar force-free fields), this is not true in the lower solar atmosphere (see Wiegelmann et al. 2014, for a recent review on magnetic fields in the solar atmosphere). In the photosphere and lower chromosphere low and high β regions exist side by side and non-magnetic forces have to be taken into account, to lowest order with a magneto-static model, where the Lorentz-force is compensated by the gradient of the plasma pressure and the gravity force.

The most accurate measurements of the solar magnetic field are available in the photosphere. In active regions the full magnetic vector can be measured accurately, e.g. with SDO/HMI, whereas in quiet Sun regions only the line-of-sight or vertical field is available with sufficient accuracy for a reliable extrapolation, because in weak field regions there is too much uncertainty in the transverse field components (Noise in the Stokes vector translate into an uncertainty in the inferred values for the magnetic field, see Borrero & Kobel 2011, 2012). These photospheric measurements are extrapolated into the solar atmosphere under certain model assumptions, here a magneto-static approach. The vertical resolution of the model scales with the horizontal resolution of the photospheric measurements, e.g. about 1400 km for SOHO/MDI-magnetograms and 350 km for SDO/HMI. As the non-force-free layer containing the photosphere and lower chromosphere is rather thin (typically less than 2000 km), one can hardly resolve magnetic struc-

tures here for models using SOHO/MDI- or SDO/HMI-magnetograms as boundary condition. The high resolution magnetograms from SUNRISE/IMaX with a pixel size of only 40 km allow now to model this layer vertically with about 50 points.

A special class of magneto-static solutions, which allow separable solutions has been proposed by Low (1991). An advantage of this approach is that the resulting equations are linear (for nonlinear cases, see Neukirch 1997) and can be solved effectively by a Fourier transformation or a Green's function implementation (see Petrie & Neukirch 2000). Separable and linear solutions have been found also in spherical (Bogdan & Low 1986; Neukirch 1995; Al-Salti & Neukirch 2010) as well as in cylindrical coordinates (Neukirch 2009; Al-Salti et al. 2010). Especially the solutions found in spherical coordinates have been used for modelling the global magnetic field of the Sun (e.g. Bagenal & Gibson 1991; Gibson & Bagenal 1995; Gibson et al. 1996; Zhao et al. 2000; Ruan et al. 2008) and other stars (e.g. Lanza 2008, 2009).

Usually these models require only the line-of-sight or vertical photospheric magnetic field as boundary condition and the solutions contain free parameters and/or free functions. Nonlinear magneto-static solutions are more demanding numerically and observationally, because they require photospheric vector magnetograms as input (see Wiegelmann & Neukirch 2006; Wiegelmann et al. 2007, for a cartesian and spherical implementation, respectively). Within this work we apply the linear magneto-static solutions proposed by Low (1991) to a high-resolution magnetogram observed with SUNRISE/IMaX. We outline the paper as follows. In section 2 we briefly discuss the basic equations and model assumptions. Section 3 describes the employed photo-

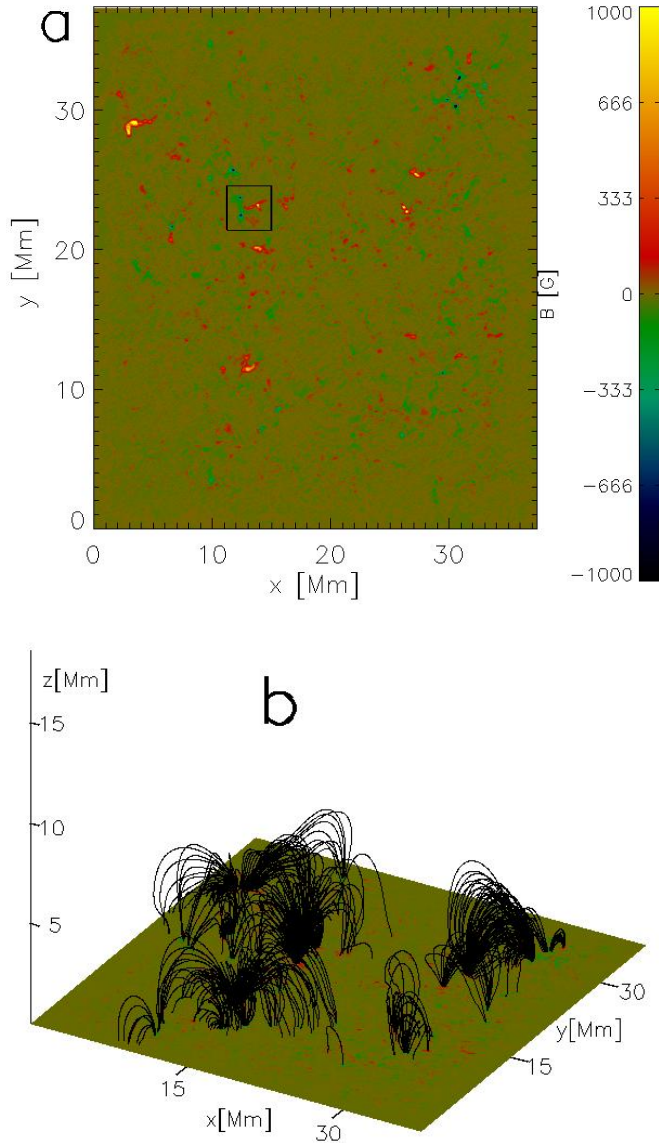


FIG. 1.— Panel a: SUNRISE/IMax magnetogram of a quiet Sun area. The black rectangular marks the region of interest. Panel b: Sample field lines for a MHS-model.

spheric magnetograms, which we use as boundary condition for our magneto-static model in section 4. In section 5 we finally discuss the prospects and limitations of this approach and give an outlook for a generalization of the method towards a non-linear numerical approach.

2. BASIC EQUATIONS

We use the magneto-hydro-static equations

$$\mathbf{j} \times \mathbf{B} = \nabla P + \rho \nabla \Psi, \quad (1)$$

$$\nabla \times \mathbf{B} = \mu_0 \mathbf{j}, \quad (2)$$

$$\nabla \cdot \mathbf{B} = 0, \quad (3)$$

where \mathbf{B} is the magnetic field, \mathbf{j} the electric current density, P the plasma pressure, ρ the mass density, Ψ the gravitational potential and μ_0 the permeability of free space. To find separable solutions for this set of equations, we apply the following ansatz for the electric cur-

rent density (see Low 1991, for details).

$$\nabla \times \mathbf{B} = \alpha_0 \mathbf{B} + f(z) \nabla B_z \times \mathbf{e}_z, \quad (4)$$

where α_0 is the force-free parameter and $f(z)$ is a free function, which controls the non-magnetic forces. The first part $\alpha_0 \mathbf{B}$ corresponds to a field-line-parallel linear force-free current and the second term $f(z) \nabla B_z \times \mathbf{e}_z$ defines a current perpendicular to the gravitational force (in the z -direction) or, in other words, parallel to the Sun's surface (x, y). It is then possible to reduce the MHS equations to a single partial differential equation (see e.g. Neukirch & Rastätter 1999, for a particularly simple formulation) that can often be solved by separation of variables. For convenience we use here (as proposed in Low 1991)

$$f(z) = a \exp(-\kappa z), \quad (5)$$

with a free parameter a , which controls the non-magnetic forces in the photosphere. Obviously, for the choice $a = 0$, this approach reduces to linear force-free fields. Above a certain height in the solar atmosphere one expects that the solution becomes approximately force-free, owing to the low plasma β in the solar corona. Consequently $f(z)$ has to decrease with height and here we choose as a scale height the distance of the upper chromosphere above the solar surface, leading to $1/\kappa = 2Mm$. With κ fixed, our MHS-solution contains two free parameters, a and a . Let us remark that κ in equation (5) controls the non-magnetic forces and should not be confused with the scale height of the plasma pressure.

As boundary conditions we use the measured vertical magnetic field $B_z(x, y, 0)$ in the photosphere. We solve the equations by means of a Fast-Fourier-Transform method similar to the linear force-free model developed by Alissandrakis (1981). Different from the linear force-free approach is that the resulting Schrödinger equation for B_z in the Fourier space contains a Bessel function instead of an exponential function

One finds the following solution for pressure and density (see Low 1991, for the derivation)

$$P = P_0(z) - \frac{1}{2\mu_0} f(z) B_z^2, \quad (6)$$

$$\rho = -\frac{1}{g} \frac{dP_0}{dz} + \frac{1}{\mu_0 g} \left[\frac{df}{dz} \frac{B_z^2}{2} + f(\mathbf{B} \cdot \nabla) B_z \right]. \quad (7)$$

The first term in equation (6) contains a 1D-solution (in z -direction), which is independent of the magnetic field and has to obey $\nabla P = -\rho \nabla \Psi$. The second term is the disturbance of this 1D-pressure profile by the magnetic field. Here pressure and density compensate the non-vanishing Lorentz-force. This disturbance is negative (if $a > 0$), and obtains its highest absolute values in regions of the highest vertical magnetic field strength B_z . Because the total plasma pressure (sum of both terms) has to be positive, we get the following in-equality for $P_0(z)$

$$P_0(z) > a \cdot \exp(-\kappa z) \cdot \frac{\text{Max}(B_z)^2}{2\mu_0}(z), \quad (8)$$

where $\frac{\text{Max}(B_z)^2}{2\mu_0}(z)$ is the maximum at a given height z . As we will see later, this condition has severe consequences for an application to data with strong locally

enhanced magnetic fields in the photosphere. To satisfy condition (8) in these regions, the background pressure P_0 has to be so high that the plasma β in weak-field regions (and also on average) becomes unrealistically high, see Fig. 3. Within this limitation, the choice of $P_0(z)$ has some freedom. Our choice is given in section 4.1.

3. DATA

We apply our newly developed code to photospheric magnetic field measurements taken with the balloon-borne SUNRISE solar observatory in June 2009. For an overview of the SUNRISE mission and scientific highlights of the first SUNRISE flight see Solanki et al. (2010), Barthol et al. (2011), Berkefeld et al. (2011), Gandorfer et al. (2011). For a description of the IMAx instrument, we refer to Martínez Pillet et al. (2011). The photospheric magnetic field was computed by inverting the IMAx measurements using the VFISV code as described in Borrero et al. (2011). The linear force-free extrapolation code, and the particular case of an $\alpha = 0$ potential field has been applied to data from SUNRISE/IMAx before for a single magnetogram by Wiegmann et al. (2010) and to analyse a time series by Wiegmann et al. (2013). Chitta et al. (2014) carried out non-linear force-free extrapolations from IMAx magnetograms and added vertical flows at low heights to simulate non-force-free effects in the photosphere and chromosphere. Here we apply our newly developed linear MHS-code to a snapshot of the quiet Sun, observed with SUNRISE/IMAx as well. We apply our code first to the full field-of-view of IMAx, as shown in Fig. 1 and in a subsequent step we investigate a subfield (marked with a black rectangular in Fig. 1) in more detail. The data set used here was observed in a period of 1.616 hours starting at 00:00 UT on 2009 June 9th (image 220 from this series), see Martínez Pillet et al. (2011).

4. RESULTS

4.1. Application to the full IMAx-FOV.

In our first computation we apply our model to the full phase-diversity reconstructed IMAx magnetogram of a quiet Sun region of 37×37 Mm, which has been resolved by 936×936 pixels (pixel size on Sun 40 km), see Fig. 1. As our main interest lies in the mixed plasma β regions of the photosphere and chromosphere, we extrapolate up to a height of $z = 4$ Mm or 100 pixels. A few sample field lines for a magneto-static solution with $\alpha = 3.0$ and $a = 0.5$ is shown in in Fig. 1 b).

In Fig. 2 a) we show the pressure disturbance in the chromosphere at the height $z = 1$ Mm as calculated with the second term $-\frac{1}{2\mu_0}f(z)B_z^2$ on the right-hand-side of Eq. (6). This term obviously becomes largest above regions with the highest photospheric field strength, as seen in the large negative peaks. The total pressure has to be positive of course and consequently a lower bound for the 1D-background pressure P_0 is given by Eq. (8). P_0 describes a 1D-equilibrium between the gravity force and the vertical pressure gradient. One has to solve:

$$\frac{dP_0(z)}{dz} = -g\rho(z) \quad (9)$$

for a constant gravity g . Assuming an equation of state

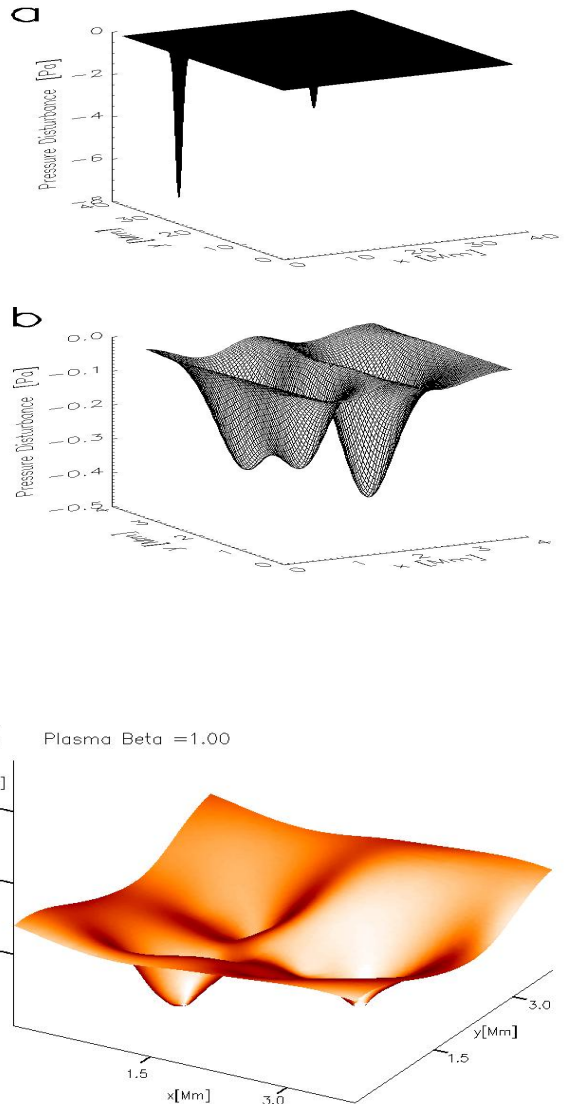


FIG. 2.— The plasma pressure disturbance $-\frac{1}{2\mu_0}f(z)B_z^2$ at a height $z = 1$ Mm for the full IMAx and the small FOV in panel a) and b), respectively. Panel c) shows an equi-contour surface for $\beta = 1$ in the small FOV.

of the form $P_0 = \rho RT$ we get

$$\frac{dP_0(z)}{dz} = -\frac{gP_0(z)}{RT}, \quad (10)$$

which leads to the well-known atmospheric exponential decay $\propto \exp(-\frac{z}{2H})$, with $H \approx 180$ km. for a constant Temperature $T = T_0$, which is, however, not realistic for describing structures reaching from the photosphere through the chromosphere into the corona. Equation (10) can be (numerically) integrated for any choice of a temperature profile $T(z)$, e.g., from 1D-models of the solar atmosphere. Another alternative is (because we computed already the 3D magnetic field from Eq. 4 and 5) to prescribe the average plasma $\beta(z)$ as a function of z , e.g. from the literature (Gary 2001), leading to

$$P_0(z) = \frac{\beta(z) B_{ave}^2}{2\mu_0} \quad (11)$$

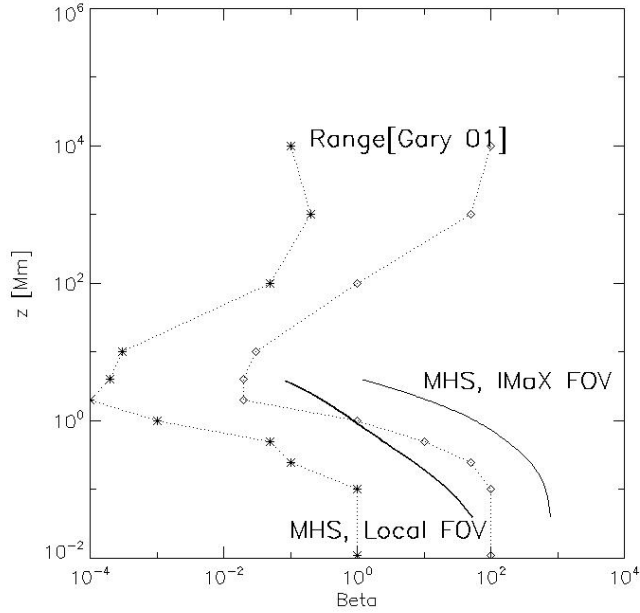


FIG. 3.— Plasma β in the solar atmosphere. The dotted lines are taken from Gary (2001). The thin solid line shows the (horizontally averaged) plasma β profile computed with our MHS-model for the full IMaX-FOV and the thick solid line represents the same for the selected small area.

where $B_{\text{ave}}(z)$ is the horizontally averaged $B_z(x, y, z)$. The allowed ranges for $\beta(z)$ are bounded from below, however, by Eq. 8. A choice which ensures a total positive pressure is obtained by using Eq. 8 directly

$$P_0(z) = P_\epsilon(z) + a \cdot \exp(-kz) \cdot \frac{\text{Max}(B_z)^2(z)}{2\mu_0}, \quad (12)$$

where $P_\epsilon(z)$ is the (prescribed) minimum value of the total pressure at a given height. For $P_\epsilon(z) = 0$ the total plasma pressure becomes zero at the maximum of B_z and remains positive elsewhere. Taking this into account we can calculate the full average plasma β (including the pressure disturbance) from Eq. (6), as shown in Fig. 3 right-most-curve labeled *MHS, IMaX FOV* in Fig. 3. The limitations from Eq. (8) and a magnetogram with some high peak values in an otherwise weak field region cause values of plasma β which are too high and outside the range given by Gary (2001) (dotted curves). We have to conclude, that the linear MHS-model cannot be applied to the whole FOV of the SUNRISE magnetogram realistically. The reason is that through Eq. (12) the 1-D background pressure and thereby the maximum pressure in weak field regions is coupled with the highest values in the photospheric magnetogram, which is not very realistic.

4.2. Application to a small part of the FOV

Due to the difficulties of applying the linear MHS-model to a full magnetogram, we restrict our analysis in the following to the smaller sub-region marked by the black rectangle in Fig. 1 a). Figure 4 shows a few sample field lines for a) a potential field model, b) a linear force-free model with $\alpha = 3$ and c) a magneto-static solution $\alpha = 3$, $a = 0.5$. In the linear force-free case the field lines become sheared compared with the potential

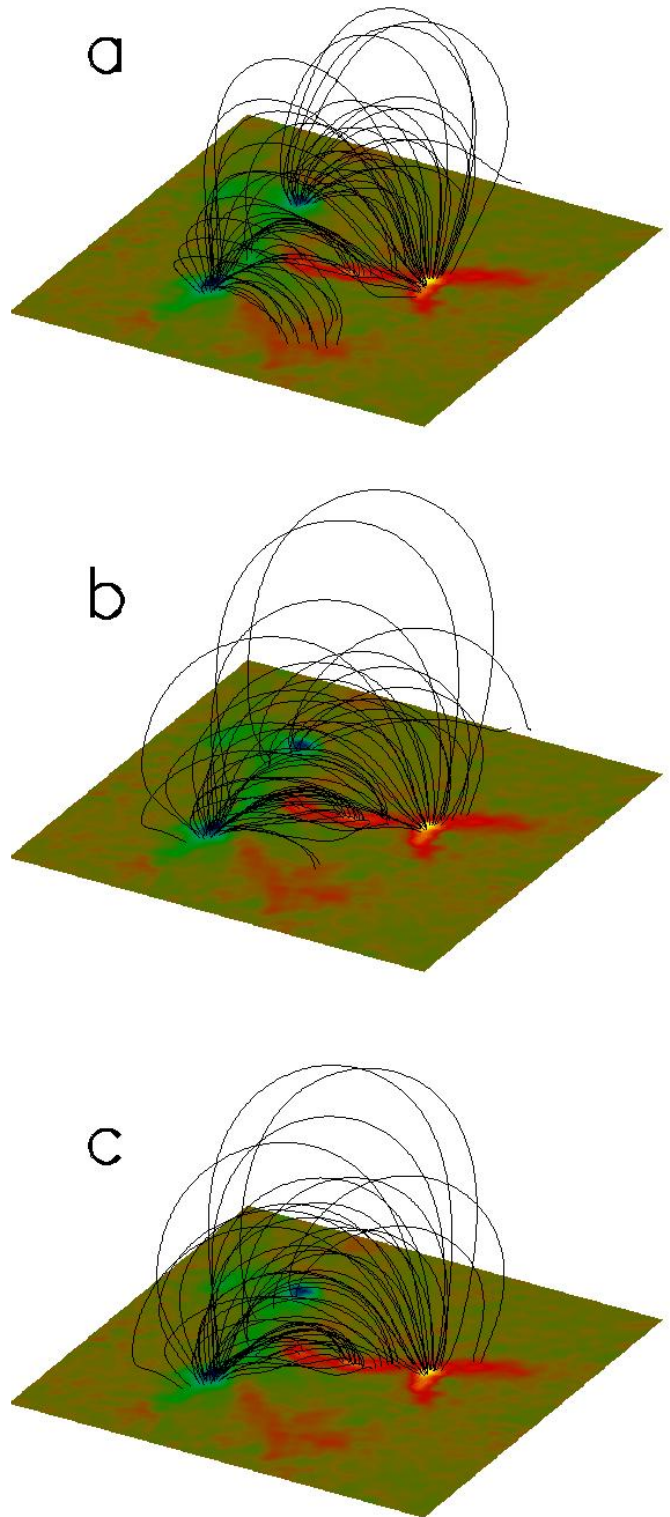


FIG. 4.— Small field of view (rectangular box in fig. 1a.) a: Potential field, b: Linear force-free field, c: magneto-static field.

field and for some lines the connectivity changes. The influence of a non-vanishing Lorentz force (but using the same value of α as in the linear force-free case) has additional effects, which seem, however, to be smaller. The maximum heights of the loops are somewhat reduced and some additional field lines change their connectivity, e.g. in the MHS-model no lines are connected with the positive (red) flux region close to the front boundary. Compared with the potential fields, the number of field lines connecting to this region was already reduced in the linear-force-free model.

The pressure-disturbance in this smaller FOV is shown in the center panel of Fig. 2. The absence of strong peaks in the photospheric field in this region leads to a much smoother distribution of the pressure disturbance. We use Eq. 12 to compute the background pressure and in Fig. 3 the solid line marked *MHS, local FOV* shows the averaged plasma β as a function of the height. At least in the photosphere and chromosphere the plasma β is within the limitation given by the dashed lines from the literature (Gary 2001). The true 3D plasma β distribution is, however, not a function of z only, but varies significantly in the horizontal direction. Fig. 2 c) shows the equi-contours for $\beta = 1.0$. As one can see the $\beta = 1.0$ surface is by no means plane-parallel, but strongly corrugated. This behaviour impacts methods for extrapolating force-free fields. Traditionally and for numerical simplicity, one extrapolates from a plane parallel surface (or the Sun's spherical surface) by assuming that the field above this lower boundary of the computational domain is force-free. In reality, however, the force-free domain is bounded below by a corrugated surface as well. This is also true for planned measurements of the chromospheric magnetic field vector with Solar-C, so that magnetic field extrapolation techniques bounded by non-plane-parallel surfaces should be developed. In the non-force-free region between the photosphere and the corrugated chromosphere, plasma pressure and gravity must be taken into account.

5. DISCUSSION AND OUTLOOK

The linear-MHS approach used in this paper has 2 free parameters, the linear-force-free parameter α and the force-parameter a . Additionally one has to prescribe, besides the vertical magnetic field component at the lower boundary, also the height in the solar atmosphere, where the magnetic field becomes approximately force-free, here $1/\kappa = 2Mm$. Applying these solutions to large-scale areas has its limitations. These are, first of all, the well-known limitations on α , which these solutions share with linear force-free configurations. Additionally the pressure-gradient (which compensates the Lorentz-force) is coupled to the vertical magnetic field. As a consequence, the pressure disturbance, which is negative, becomes very large above strong fields in the photosphere. In order to maintain a positive total pressure, the background plasma pressure must be so strong that the average plasma β becomes too high. This limitation of the method has to do with the fact that the two free parameters α and a have to be the same in the entire computational domain. The limitations are similar as for linear force-free fields, where one has only one free

parameter α , which has to be globally constant. While linear force-free fields cannot be used to model force-free configurations containing strong current concentrations in part of the domain (leading to localized high values of α), a similar restriction occurs here for the linear magneto-static approach. Strong magnetic elements in an otherwise weak field magnetogram cannot be modelled by this class of MHS solutions.

These limitations do not occur, however, for application to regions with a smaller field of view, because the assumption that α and a are constant is naturally more reasonable as smaller the investigated domain is. How should one proceed to derive global magneto-static solutions? One possibility would be to compute the solutions discussed here only locally (with different values of α and a in different regions) and to merge these configurations together. This will of course lead to solutions which are not entirely self-consistent and to inconsistencies at the boundaries between the different regions. Another idea would be to use a numerical scheme, e.g. an optimization approach as suggested by Wiegelmann & Neukirch (2006), Wiegelmann et al. (2007) to relax these merged solutions towards a self-consistent (non-linear) MHS-equilibrium. The methods developed by Wiegelmann & Neukirch (2006) and Wiegelmann et al. (2007) are both non-linear magneto static codes in cartesian and spherical geometry, respectively. For the small scale features measured with Sunrise, one naturally applies the cartesian version. These codes require photospheric vector magnetograms as input, which are not available for the investigated quiet Sun region, because of the poor signal to noise ratio (for horizontal fields) in weak field regions. Nonlinear approaches (both force-free and magneto static) are well suited for dealing with local strong enhancements (e.g. current concentrations and strong flux elements). It is a weakness of any linear approach, that they cannot deal with strong localized enhancements of any quantity.

To be able to carry out nonlinear magnetostatic (or nonlinear force-free) extrapolations, measurements of the horizontal photospheric magnetic field, would be helpful. During the re-flight of SUNRISE in 2013, high resolution vector magnetograms of active region(s) have been measured with IMA \bar{X} and we plan to use these measurements for a self-consistent nonlinear magneto-static modelling in our future work.

The German contribution to *SUNRISE* is funded by the Bundesministerium für Wirtschaft und Technologie through Deutsches Zentrum für Luft- und Raumfahrt e.V. (DLR), Grant No. 50 OU 0401, and by the Innovationsfonds of the President of the Max Planck Society (MPG). The Spanish contribution has been funded by the Spanish MICINN under projects ESP2006-13030-C06 and AYA2009-14105-C06 (including European FEDER funds). The HAO contribution was partly funded through NASA grant number NNX08AH38G. TN acknowledges support by the U.K.'s Science and Technology Facilities Council and would like to thank the MPS for its hospitality during a visit in December 2014. D.H.N. acknowledges financial support from GA ĆR under grant number 13-24782S. The Astronomical Institute Ondřejov is supported by the project RVO:67985815.

REFERENCES

- Al-Salti, N. & Neukirch, T. 2010, *A&A*, 520, A75
Al-Salti, N., Neukirch, T., & Ryan, R. 2010, *A&A*, 514, A38
Alissandrakis, C. E. 1981, *A&A*, 100, 197
Bagenal, F. & Gibson, S. 1991, *J. Geophys. Res.*, 96, 17663
Barthol, P., Gandorfer, A., Solanki, S. K., et al. 2011, *Sol. Phys.*, 268, 1
Berkefeld, T., Schmidt, W., Soltau, D., et al. 2011, *Sol. Phys.*, 268, 103
Bogdan, T. J. & Low, B. C. 1986, *ApJ*, 306, 271
Borrero, J. M. & Kobel, P. 2011, *A&A*, 527, A29
Borrero, J. M. & Kobel, P. 2012, *A&A*, 547, A89
Borrero, J. M., Tomczyk, S., Kubo, M., et al. 2011, *Sol. Phys.*, 273, 267
Chitta, L. P., Kariyappa, R., van Ballegoijen, A. A., DeLuca, E. E., & Solanki, S. K. 2014, *ApJ*, 793, 112
Gandorfer, A., Grauf, B., Barthol, P., et al. 2011, *Sol. Phys.*, 268, 35
Gary, G. A. 2001, *Sol. Phys.*, 203, 71
Gibson, S. E. & Bagenal, F. 1995, *J. Geophys. Res.*, 100, 19865
Gibson, S. E., Bagenal, F., & Low, B. C. 1996, *J. Geophys. Res.*, 101, 4813
Lanza, A. F. 2008, *A&A*, 487, 1163
Lanza, A. F. 2009, *A&A*, 505, 339
Low, B. C. 1991, *ApJ*, 370, 427
Martínez Pillet, V., Del Toro Iniesta, J. C., Álvarez-Herrero, A., et al. 2011, *Sol. Phys.*, 268, 57
Neukirch, T. 1995, *A&A*, 301, 628
Neukirch, T. 1997, *A&A*, 325, 847
Neukirch, T. 2009, *Geophysical and Astrophysical Fluid Dynamics*, 103, 535
Neukirch, T. & Rastätter, L. 1999, *A&A*, 348, 1000
Petrie, G. J. D. & Neukirch, T. 2000, *A&A*, 356, 735
Ruan, P., Wiegelmann, T., Inhester, B., et al. 2008, *A&A*, 481, 827
Solanki, S. K., Barthol, P., Danilovic, S., et al. 2010, *ApJ*, 723, L127
Wiegelmann, T. & Neukirch, T. 2006, *A&A*, 457, 1053
Wiegelmann, T., Neukirch, T., Ruan, P., & Inhester, B. 2007, *A&A*, 475, 701
Wiegelmann, T. & Sakurai, T. 2012, *Living Reviews in Solar Physics*, 9, 5
Wiegelmann, T., Solanki, S. K., Borrero, J. M., et al. 2010, *ApJ*, 723, L185
Wiegelmann, T., Solanki, S. K., Borrero, J. M., et al. 2013, *Sol. Phys.*, 283, 253
Wiegelmann, T., Thalmann, J. K., & Solanki, S. K. 2014, *A&A Rev.*, 22, 78
Zhao, X. P., Hoeksema, J. T., & Scherrer, P. H. 2000, *ApJ*, 538, 932